

Mixed columnar-plaquette phase of hard-core bosons and its quantum melting

Stefan Wessel

Institut für Theoretische Physik III, Universität Stuttgart, Pfaffenwaldring 57, 70550 Stuttgart, Germany

(Received 18 June 2008; revised manuscript received 31 July 2008; published 18 August 2008)

We examine the ground-state phase diagram of repulsively interacting hard-core bosons on the quarter-filled checkerboard lattice using quantum Monte Carlo simulations constrained to the canonical ensemble. At a sufficiently large repulsion, the system undergoes a quantum phase transition from a superfluid into a valence-bond-solid regime. We identify this as a weakly first-order quantum melting transition at quarter filling. Furthermore, by examining appropriate order parameters, we exhibit the mixed nature of the valence bond solid, with both columnar and plaquette long-ranged order. Our results demonstrate the realization of the mixed columnar-plaquette phase found recently for the square lattice quantum dimer model in a microscopic bosonic system.

DOI: 10.1103/PhysRevB.78.075112

PACS number(s): 71.27.+a, 05.30.Jp, 75.10.Jm, 75.40.Mg

I. INTRODUCTION

In search for exotic quantum phases and unconventional quantum phase transitions, lattice models of hard-core bosons with short-ranged repulsions are being intensively studied recently. Such models can exhibit order-by-disorder phenomena if quantum fluctuations lift an extensive ground-state degeneracy from the classical limit, and new quantum phases emerge. Examples include supersolid phases in the case of the triangular lattice,¹⁻⁴ valence bond solids,^{5,6} a Z_2 spin liquid⁷⁻⁹ on the kagome lattice, and a $U(1)$ liquid on the pyrochlore lattice.¹⁰ In the limit of dominant kinetic terms, these systems stabilize a superfluid phase on both bipartite and nonbipartite lattices. The quantum phase transition between a superfluid and a valence bond solid, which breaks the space-group symmetry, would be expected to be generically first order within Landau's theory of phase transitions. However, in recent analytical scenarios, some of these transitions have been conjectured to fall outside this framework, and to establish examples of Landau-forbidden second-order quantum phase transitions.^{11,12}

Based on gauge theory considerations, such conclusions were reached also for interacting hard-core bosons on the checkerboard lattice at quarter filling.¹³ This was, however, in contrast to quantum Monte Carlo (QMC) results reported by the same authors, which indicated a weakly first-order transition near quarter filling.¹³ The definite nature of the insulating phase emerging in this model also remained unclear. As detailed below, one might expect that in this model a mixed phase exhibiting both columnar and plaquette ordering could be realized; such expectation is based on a recent study¹⁴ on the square lattice quantum dimer model,¹⁵ which effectively describes the restricted dynamics in the hard-core boson model for dominant repulsions.¹⁴ Indeed, in Ref. 14, it was concluded that such a mixed columnar-plaquette phase exists in the relevant parameter range of the quantum dimer model.

Motivated by these investigations, we here present results from QMC simulations on this model of hard-core bosons on the checkerboard lattice, constrained to exactly quarter filling. Our simulations were performed using the generalized directed loop^{16,17} stochastic series expansion^{18,19} algorithm

with a plaquette decoupling, in the effective ground state of finite systems with up to $N=L \times L=60 \times 60$ lattice sites (we found that temperatures $T=0.55 J/L$ were necessary in order to assure that ground-state properties were obtained). As presented in detail below, we conclude from our numerical investigation that (i) indeed the valence bond solid in this model exhibits a mixed nature of both columnar and plaquette ordering, and (ii) this state melts at a weakly first-order quantum phase transition into the superfluid phase also at fixed quarter filling, i.e., through the tip of the quarter-filled insulator lobe in a grand-canonical phase diagram.¹³

II. BOSONS AND QUANTUM DIMER MODELS

In the following, we analyze the ground-state properties of the hard-core extended boson Hubbard model

$$H = -J \sum_{\langle i,j \rangle} (b_i^\dagger b_j + b_j^\dagger b_i) + V \sum_{\langle i,j \rangle} n_i n_j + V \sum_{\langle\langle i,j \rangle\rangle} n_i n_j \quad (1)$$

on the checkerboard lattice shown in Fig. 1(a). Here, b_i^\dagger (b_i) denote creation (annihilation) operators for hard-core bosons on lattice site i , and $n_i = b_i^\dagger b_i$ the local-density operator; J is the nearest-neighbor hopping amplitude, and V a repulsion that acts along the nearest-neighbor bonds and also the next-nearest-neighbor bonds (red lines in Fig. 1) of the filled plaquettes (clusters) of the checkerboard lattice.

In the canonical ensemble the above Hamiltonian equals, up to a constant, the cluster-charging model

$$H = -J \sum_{\langle i,j \rangle} (b_i^\dagger b_j + b_j^\dagger b_i) + \frac{V}{2} \sum_p (n_p - 1)^2 \quad (2)$$

expressed in terms of the cluster charges (densities)

$$n_p = n_{p1} + n_{p2} + n_{p3} + n_{p4}, \quad (3)$$

on cluster p , where n_{pi} , $i=1,2,3,4$ are the density operators on the four sites that form cluster p , as indicated for the central cluster in Fig. 1(a).

In the atomic limit $J=0$, the ground-state manifold at quarter filling is spanned by all configurations, for which each cluster is occupied by exactly one boson, $n_p=1$. As is well known, these configurations can be mapped onto hard-

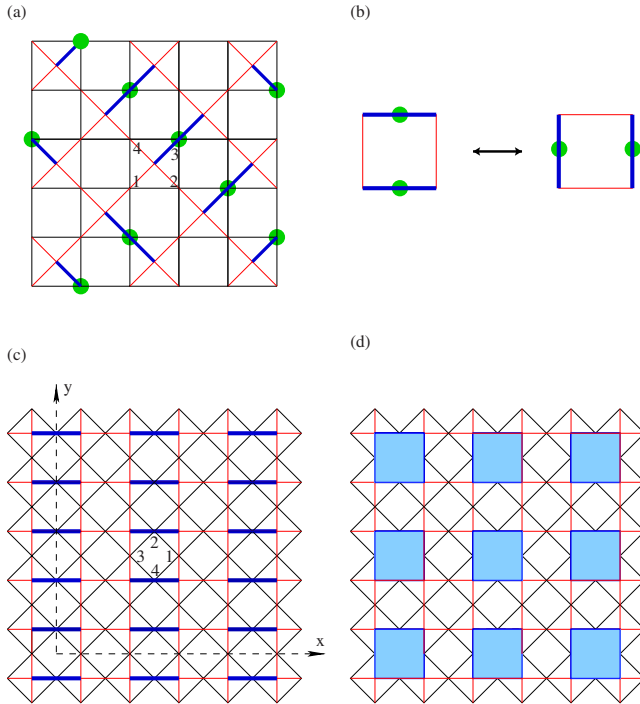


FIG. 1. (Color online) (a) Hard-core bosons (circles) on the checkerboard lattice, and mapping to a dimer (bold blue/dark gray lines) covering of the square lattice (red/gray lines). (b) The local flip move of two parallel dimers along a void plaquette. (c) The ideal columnar state of the quantum dimer model on the square lattice. (d) The ideal plaquette state of the quantum dimer model on the square lattice, with each filled square indicating the local resonance shown in part (b).

core dimer coverings of the square lattice formed by the diagonal bonds in the checkerboard lattice, namely, by assigning a dimer to each bond passing through a site that is occupied by a boson, as illustrated in Fig. 1(a). A finite hopping amplitude $J \neq 0$ induces quantum tunneling between states from the classical ground-state manifold. The leading-order effective Hamiltonian in the limit $J/V \rightarrow 0$ is a quantum dimer model with resonance terms that flip two parallel dimers on a square lattice plaquette from the vertical to the horizontal orientation, and vice versa [cf. Fig. 1(b)],

$$H_t = -t \sum_{(C,C')} |C\rangle\langle C'|. \quad (4)$$

Here, the sum runs over all pairs of dimer coverings (C, C') that differ by a single flip of two parallel dimers on a square lattice plaquette, and $t = O(J^2/V)$. The above Hamiltonian is a special point in the more general Rokhsar-Kivelson (RK) quantum dimer model,¹⁵ that includes in addition to the above kinetic term also a competing potential term,

$$H_w = -t \sum_{(C,C')} |C\rangle\langle C'| + v \sum_C N_{fp}(C) |C\rangle\langle C|, \quad (5)$$

where $N_{fp}(C)$ denotes the number of flippable plaquettes in configuration C (in bosonic language this potential term relates to additional interactions between bosons along the diagonals of all void plaquettes of the checkerboard lattice).

The above Hamiltonian includes the special RK point at $v = t$, where the system can be solved exactly, and has a critical dimer liquid ground state, formed by the equally weighted superposition of all dimer coverings.¹⁵

The ground-state phase diagram of the above Hamiltonian has been the subject of several investigations. For $v/t > 1$ the system is in a staggered dimer ground state, whereas at sufficiently negative v/t a columnar state illustrated in Fig. 1(c) is stabilized.^{15,20} Regarding the intermediate region $-0.2 \lesssim v/t < 1$, including the point $v/t = 0$ of the hard-core bosonic model in the form of Eq. (1), previous studies led to differing conclusions. Leung *et al.*,²¹ based on exact diagonalizations, find indications for a transition at $v/t \approx -0.2$ from the columnar phase to a phase with disorder in the columnar arrangement, consistent with a plaquette state, illustrated in Fig. 1(d). Syljuåsen,²² using quantum Monte Carlo, locates the transition from the columnar to the plaquette phase at a significantly larger value of $v/t \approx 0.6$. Ralko *et al.*¹⁴ suggest these findings to be reconciled in a scenario resulting from combining a symmetry analysis of the ground-state manifold based on exact diagonalization and Green's function Monte Carlo with effective-field theory considerations. The authors obtain a strong indication for a mixed phase in the region $0.0 \lesssim v/t \lesssim 0.6$, which interpolates between the columnar and plaquette phases. In contrast to the columnar and plaquette states, both of which are fourfold degenerate, this mixed phase has an eightfold degenerate ground-state manifold.¹⁴ Evidence in favor of such a scenario comes from the finite-size scaling of the excitation gaps to the corresponding degenerate ground-state manifold in the thermodynamic limit, as well as structure factors of appropriate plaquette operators, which target specific symmetry-breaking sectors.¹⁴ In the following, we employ the equivalent bosonic versions of these order parameters to establish the presence of a mixed phase also in the hard-core bosonic model of Eq. (1). With respect to the quantum dimer model, our results can thus be interpreted in favor of a mixed phase at $v/t = 0$.

III. MIXED PHASE

As already noted in Ref. 13 the model in Eq. (1) exhibits a quantum phase transition from a superfluid phase at dominant hopping J to an insulating phase for V/J beyond a critical value, which we determine to be $(V/J)_c = 6.35(1)$ at quarter filling. This transition is clearly seen in Fig. 2 from monitoring the superfluid density ρ_S as a function of V/J . In the QMC simulations, ρ_S is obtained²³ as

$$\rho_S = T \langle W^2 \rangle / (2J) \quad (6)$$

from monitoring the boson winding number fluctuations $\langle W^2 \rangle$. Also shown in Fig. 2 is the fraction f_1 that gives the relative number of clusters (nonvoid plaquettes) that are occupied by a single boson. Inside the superfluid regime, f_1 follows a linear increase with V/J , and exhibits sublinear behavior inside the insulating phase, where it saturates toward unity for $J \rightarrow 0$. Indeed, in the limit $J = 0$ we get $f_1 = 1$, corresponding to the single-occupation constraint on each cluster, from the discussion in Sec. II. We find that within the

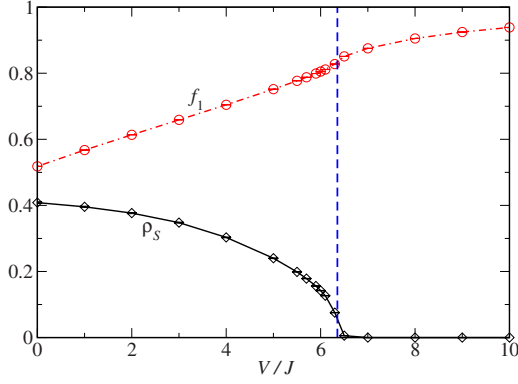


FIG. 2. (Color online) Superfluid density ρ_s and the fraction f_1 , which gives the relative number of singly occupied clusters (non-void plaquettes) for hard-core bosons on the checkerboard lattice at quarter filling as a function of V/J . Data from QMC simulations of a $L=28$ system are shown.

insulating regime more than 85% of the clusters on average fulfill this single-occupation constraint that holds also in the quantum dimer model limit of this model, and for $V/J > 10$, this percentage has increased beyond 95%. This can be taken as an indication that the quantum dimer model can provide a description of the low-energy physics of this model over a large extent of the insulating regime, and motivates our search for a mixed phase in the bosonic model.

In order to establish the nature of the insulating phase, Sen *et al.*¹³ employed two complex order parameters formed from local-density and kinetic-energy operators, respectively. In the notation of Fig. 1(c), the density based order parameter is given by

$$\psi_c = n_1(\pi, 0) + in_2(0, \pi), \quad (7)$$

in terms of the density Fourier transforms

$$n_\alpha(\mathbf{q}) = \frac{1}{N_v} \sum_{i=1}^{N_v} e^{i\mathbf{q}\cdot\mathbf{r}_i} n_{i\alpha}, \quad (8)$$

where the summation is performed over all $N_v = N/2$ void plaquettes, and $n_{i\alpha}$ is the local bosonic density operator on lattice site $\alpha = 1, \dots, 4$ within plaquette i , according to the site labeling along each void plaquette, as illustrated for the central plaquette in Fig. 1(c). The integer coordinates $\mathbf{r}_i = (x_i, y_i)$ of plaquette i are taken with respect to the coordinate system indicated in Fig. 1(c). This order parameter is sensitive to spatial symmetry breaking in the insulating phase.¹³ The inset of Fig. 3 shows the dependence of the QMC expectation value of the magnitude of the order parameter, $|\psi_c|^2$, as a function of V/t across the quantum phase transition for different system sizes [L denotes the linear extent of the cluster with periodic boundary conditions in each direction, so the number of lattice sites $N = L^2$, and the cluster shown in Fig. 1(a) corresponds to $L=6$]. The finite magnitude $|\psi_c|^2$ in the insulating phase reveals that translational symmetry by one lattice spacing is broken in at least one lattice direction. One might expect to access more detailed information about the spatial symmetry breaking from the phase of ψ_c . A direct calculation of ψ_c for the perfect colum-

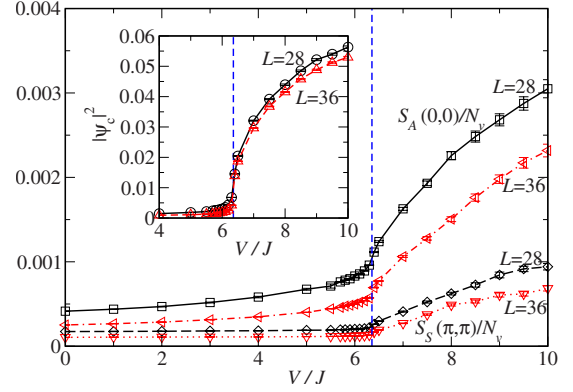


FIG. 3. (Color online) Plaquette operator based structure factors $S_S(\pi, \pi)$ and $S_A(0, 0)$ as functions of V/J for different system sizes. The inset shows the magnitude of the complex order parameter $|\psi_c|^2$ vs V/J . The location of the quantum phase transition is indicated by vertical dashed lines.

nar and plaquette states, however, reveals that this order parameter does not allow for a distinction between columnar and plaquette ordering in a Monte Carlo simulation. In particular, depending on the orientation of the dimers (horizontal vs vertical) in a columnar state, ψ_c is either purely real or purely imaginary. In the plaquette state, both real and imaginary parts take on equal finite values. Hence, neither the magnitude nor the phase of ψ_c can, in an ergodic simulation, provide more distinctive information about the type of symmetry breaking, i.e., (i) rotational plus translational in one direction (columnar state), or (ii) translational in two perpendicular directions (plaquette state), or (iii) both rotational and translational in two perpendicular directions (mixed state). Indeed, in Ref. 13 no such absolute phase information for ψ_c could be extracted from the quantum Monte Carlo simulations.

In order to probe more specifically the ordering pattern, we employ two diagonal order parameters that are constructed following Ref. 14 in terms of the symmetric and antisymmetric plaquette operators

$$\begin{aligned} P_S(i) &= n_{i1}n_{i3} + n_{i2}n_{i4}, \\ P_A(i) &= n_{i1}n_{i3} - n_{i2}n_{i4}, \end{aligned} \quad (9)$$

for each $i = 1, \dots, N_v$ of the N_v void plaquettes, again within the notation of Fig. 1(b). For both plaquette operators, we define corresponding structure factors

$$\begin{aligned} S_S(\mathbf{q}) &= \frac{1}{N_v} \sum_{i,j=1}^{N_v} e^{i\mathbf{q}\cdot(\mathbf{r}_i - \mathbf{r}_j)} P_S(i) P_S(j), \\ S_A(\mathbf{q}) &= \frac{1}{N_v} \sum_{i,j=1}^{N_v} e^{i\mathbf{q}\cdot(\mathbf{r}_i - \mathbf{r}_j)} P_A(i) P_A(j). \end{aligned} \quad (10)$$

From an explicit calculation, one finds that in the thermodynamic limit, $S_A(0, 0)/N_v$ remains finite in the columnar state, but vanishes in the pure plaquette phase, where rotational symmetry is restored. Furthermore, $S_S(\pi, \pi)/N_v$ remains finite for a plaquette state with bidirectional breaking of trans-

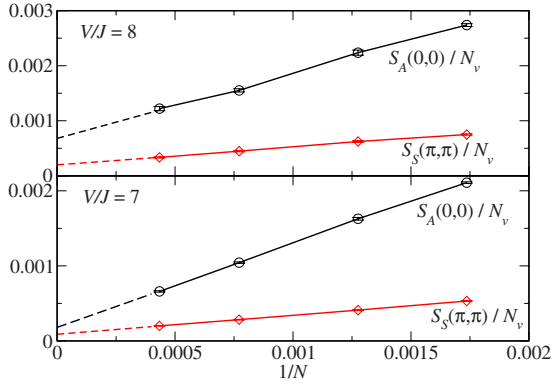


FIG. 4. (Color online) Finite-size dependence of the plaquette order based structure factors $S_S(\pi, \pi)$ and $S_A(0,0)$ for different values of V/J .

lation symmetry, but vanishes in the pure columnar state, where translation symmetry is partially restored. As in Ref. 14, we take the corresponding finite values as an indication for a generic columnar [$S_A(0,0)/N_v$] and plaquette [$S_S(\pi, \pi)/N_v$] states. In the main panel of Fig. 3 both structure factors are shown across the quantum phase transition. A finite-size analysis reveals that *both* order parameters scale to finite values in the thermodynamic limit for $V/J > 6.35$ (we do not find indications for any intermediate phase). This is shown in Fig. 4 for $V/J=8$ and 7, closer to the quantum critical point. From this we conclude that the insulating phase is characterized by the simultaneous breaking of bidirectional translational and rotational symmetry, as characteristic for a columnar-plaquette mixed phase.¹⁴ This conclusion is consistent with the QMC results¹³ for the kinetic-energy correlation function, which exhibits Bragg peaks that are in fact in accord with both a pure plaquette and a plaquettelike (e.g., mixed) state.

IV. QUANTUM MELTING TRANSITION

The analytical calculations in Ref. 13 suggested that the quantum phase transition between the superfluid and insulating phases to be a Landau-forbidden continuous unconventional transition through the tip of the insulating lobe, i.e., along the line of constant density $n=1/4$. However, QMC simulations¹³ close to the tip of the lobe gave indications for a weakly first-order transition from a histogram analysis of the order parameter $|\psi_c|^2$. In order to assess if such behavior indeed persists up to the tip of the lobe, we performed the same histogram analysis of this robust order parameter also in our simulations at fixed density $n=1/4$. The resulting histograms are shown in Fig. 5. While the histograms for the $L=40$ system in the inset do not exhibit any clear double-peak structure within the numerical resolution across the transition point, we eventually obtain an indication for such a double-peak structure for the largest system size for which we performed our simulations ($L=60$) in the main panel of Fig. 5. Only for this range of system sizes does the first-order nature of the quantum melting transition becomes visible. We thus conclude that the phase boundary between the $n=1/4$ mixed phase and the superfluid is first order everywhere.

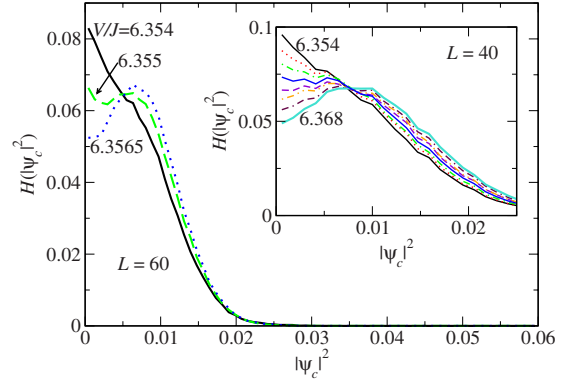


FIG. 5. (Color online) Histogram of the magnitude of the density based order parameter $|\psi_c|^2$ for the $L=60$ system for different values of V/J close to the quantum phase-transition point. The inset shows the histograms for the $L=40$ system, for values of $V/J = 6.354, 6.356, \dots, 6.568$.

V. CONCLUSIONS

Based on quantum Monte Carlo simulations constrained to the canonical ensemble, we reanalyzed the nature of the insulating phase and the quantum phase transition to the superfluid of hard-core bosons on the checkerboard lattice at quarter filling. Employing appropriate order parameters, we established the insulating regime as a mixed columnar-plaquette phase; it connects to the mixed phase found recently for the quantum dimer model on the square lattice.¹⁴ It would be interesting for the future to study finite temperature properties of the mixed phase, in particular the restoration of rotation and translation symmetry at its thermal melting transition(s). Diagonal interactions on the void plaquettes of the checkerboard lattice relate to the diagonal part of the quantum dimer model, and could be included in order to estimate the extent of the mixed phase. It will also be important to search for similar mixed phases in the fermionic analog model.²⁴ We found the quantum melting transition of the mixed phase to remain weakly first order also through the tip of the insulator lobe. The interpretation of the gauge theory considerations¹³ for this transition strongly relies on properties of the three-dimensional (easy plane) noncompact CP^1 model.²⁵ Currently, such classical models are being intensively discussed.^{25–30} One might take our quantum Monte Carlo result of a first-order transition as further evidence for the absence²⁶ of a continuous transition in the easy-plane noncompact CP^1 model. Similarly, one could test if the quantum melting transition of the valence bond crystals of hard-core bosons on the kagome lattice^{5,6} at fillings $n=1/3$ and $n=2/3$ also remains weakly first order through the tips of the lobes.

ACKNOWLEDGMENTS

We would like to thank R. Moessner and D. Poilblanc for helpful discussions, and NIC Jülich and HRLS Stuttgart for allocation of CPU time. The employed numerical simulation code is partially based on the ALPS libraries.³¹

- ¹G. Murthy, D. Arovas, and A. Auerbach, Phys. Rev. B **55**, 3104 (1997).
- ²S. Wessel and M. Troyer, Phys. Rev. Lett. **95**, 127205 (2005).
- ³R. G. Melko, A. Paramekanti, A. A. Burkov, A. Vishwanath, D. N. Sheng, and L. Balents, Phys. Rev. Lett. **95**, 127207 (2005).
- ⁴D. Heidarian and K. Damle, Phys. Rev. Lett. **95**, 127206 (2005).
- ⁵S. V. Isakov, S. Wessel, R. G. Melko, K. Sengupta, and Yong Baek Kim, Phys. Rev. Lett. **97**, 147202 (2006).
- ⁶K. Damle and T. Senthil, Phys. Rev. Lett. **97**, 067202 (2006).
- ⁷L. Balents, M. P. A. Fisher, and S. M. Girvin, Phys. Rev. B **65**, 224412 (2002).
- ⁸D. N. Sheng and L. Balents, Phys. Rev. Lett. **94**, 146805 (2005).
- ⁹S. V. Isakov, Y. B. Kim, and A. Paramekanti, Phys. Rev. Lett. **97**, 207204 (2006).
- ¹⁰A. Banerjee, S. V. Isakov, K. Damle, and Y. B. Kim, Phys. Rev. Lett. **100**, 047208 (2008).
- ¹¹T. Senthil, A. Vishwanath, L. Balents, S. Sachdev, and M. P. A. Fisher, Science **303**, 1490 (2004).
- ¹²T. Senthil, L. Balents, S. Sachdev, A. Vishwanath, and M. P. A. Fisher, Phys. Rev. B **70**, 144407 (2004).
- ¹³A. Sen, K. Damle, and T. Senthil, Phys. Rev. B **76**, 235107 (2007).
- ¹⁴A. Ralko, D. Poilblanc, and R. Moessner, Phys. Rev. Lett. **100**, 037201 (2008).
- ¹⁵D. S. Rokhsar and S. A. Kivelson, Phys. Rev. Lett. **61**, 2376 (1988).
- ¹⁶O. F. Syljuåsen and A. W. Sandvik, Phys. Rev. E **66**, 046701 (2002).
- ¹⁷F. Alet, S. Wessel, and M. Troyer, Phys. Rev. E **71**, 036706 (2005).
- ¹⁸A. W. Sandvik and J. Kurkijärvi, Phys. Rev. B **43**, 5950 (1991).
- ¹⁹A. W. Sandvik, Phys. Rev. B **59**, R14157 (1999).
- ²⁰S. Sachdev, Phys. Rev. B **40**, 5204 (1989).
- ²¹P. W. Leung, K. C. Chiu, and K. J. Runge, Phys. Rev. B **54**, 12938 (1996).
- ²²O. F. Syljuåsen, Phys. Rev. B **73**, 245105 (2006).
- ²³E. L. Pollock and D. M. Ceperley, Phys. Rev. B **36**, 8343 (1987).
- ²⁴D. Poilblanc, Phys. Rev. B **76**, 115104 (2007).
- ²⁵O. I. Motrunich and A. Vishwanath, Phys. Rev. B **70**, 075104 (2004).
- ²⁶A. Kuklov, N. Prokofev, B. Svistunov, and M. Troyer, Ann. Phys. (N.Y.) **321**, 1602 (2006).
- ²⁷O. I. Motrunich and A. Vishwanath, arXiv:0805.1494 (unpublished).
- ²⁸A. B. Kuklov, M. Matsumoto, N. V. Prokof'ev, B. V. Svistunov, and M. Troyer, Phys. Rev. Lett. **101**, 050405 (2008).
- ²⁹F. Alet, G. Misguich, V. Pasquier, R. Moessner, and J. L. Jacobsen, Phys. Rev. Lett. **97**, 030403 (2006).
- ³⁰D. Charrier, F. Alet, and P. Pujol, arXiv:0806.0559 (unpublished).
- ³¹F. Albuquerque *et al.*, ALPS Collaboration, J. Magn. Magn. Mater. **310**, 1187 (2007).